Theoret. Chim. Acta (Berl.) 47, 283–296 (1978)

THEORETICA CHIMICA ACTA

Application of a Screened INDO Model (INDO/S) to Spectroscopic Properties of TCNQ and Its Anions

Karsten Krogh-Jespersen*

Department of Chemistry, New York University, New York, N. Y. 10003, USA

Mark A. Ratner

Department of Chemistry and Materials Research Center, Northwestern University, Evanston, Illinois 60201, USA

An INDO model Hamiltonian, incorporating screening within the π-system and parametrized particularly to describe dynamical properties (photoemission and optical spectra), is applied to TCNQ and its mono- and dianion. The description of the photoelectron spectrum, the optical excitation spectra with their oscillator strengths, and the charge distributions, ground state as well as excited state, turn out reasonably well, although some difficulties are encountered with the highly charged species. A correlation between bond order changes and the frequency changes of vibrational normal modes as observed by resonance Raman spectroscopy is attempted.

Key words: Screened INDO model – TCNQ and its anions – Resonance Raman spectroscopy

1. Introduction

Our aim in developing the present INDO/S model was to follow the general NDO procedure [1, 2], but, if possible, to produce a model Hamiltonian which is applicable to a wide range of problems, minimally including optical and photoelectron spectra, multiplet splittings, oscillator strengths, and excited state charge and bond order matrices; further ground state information, if reliable, was to be a secondary benefit. There is good reason to assume that photoelectron spectra (PES) and optical spectra (UV-Vis) should be describable by the same parametrized semiempirical model, since both occur on timescales ($\lesssim 10^{-15}$ sec) short compared to vibrational times. Thermochemical, polarographic redox potential

* Present address: Institut für Organische Chemie der Universität Erlangen-Nürnberg, D-8520 Erlangen, Federal Republic of Germany

0040–5744/78/0047/0283/$02.80

as well as magnetic resonance measurements, on the other hand, are obtained on slower timescales. These slow phenomena, then, are essentially adiabatic processes, both with respect to the relaxation of the electronic wavefunction and equilibration of the nuclei. Conversely, the PES and UV-Vis results are essentially sudden perturbations with respect to vibrations and are rapid even with respect to electronic reorganization; these facts are responsible for the applicability of the Franck-Condon principle [3] and Koopmans' theorem [4], respectively. The resulting need for different parameters is for example clearly shown in the widely varying "best" values of the β parameter in the Hückel model [5] ($|\beta| = 2.71$ eV for UV-Vis, but $|\beta| = 2.27$ eV for polarography, 0.69 eV for delocalization energy).

In Sect. 2 of the present paper we describe the procedures used to calculate the ground and excited state properties as well as the actual parametrization of the Hamiltonian. Section 3 presents applications to tetracyanoquinodimethane and its anions, and Sect. 4 contains some concluding remarks.

2. The Model and Its Parametrization

We write the electronic Hamiltonian within the INDO model in the following way

$$H(\mathrm{INDO}) = \sum_{r} h_{rr} a_r^\dagger a_r + \sum_{\substack{r,s \\ A \neq B}} \beta_{rs} a_{r_A}^\dagger a_{s_B} + 0.5 \sum_{r,s} (rr|ss) a_r^\dagger a_r (a_s^\dagger a_s - \delta_{rs}) - 0.5 \sum_{\substack{r,s \\ \text{on A} \\ r \neq s}} (rs|sr) a_r^\dagger a_r a_s^\dagger a_s \tag{1}$$

Here, $a_{r_A}^\dagger (a_{r_A})$ creates (destroys) an electron in valence orbital r on atom A, and δ_{rs} is the Kronecker delta. When recipes have been devised for the evaluation of the integrals h_{rr}, β_{rs}, $(rr|ss)$, and $(rs|sr)$, solution of the Hartree-Fock equations for the electronic ground state will provide a set of orthonormal molecular orbitals and corresponding eigenvalues to be used also as input for the calculations on the excited states. In accord with Koopmans' theorem we can attempt to correlate the transitions in the experimental photoelectron spectrum to specific SCF molecular orbitals.

The molecular electronic excitation energies and the associated oscillator strengths are calculated from two schemes, the singly excited configuration interaction (SECI) approximation and the time-dependent Hartree-Fock (TDHF) approximation. Full details on these methods have been given, e.g., in the series of articles by Linderberg, Öhrn, and Jørgensen [3, 6]. To construct and diagonalize the energy matrices we take advantage of molecular symmetry, leading to considerable reduction in computer time. We utilize the Linderberg relation [7] to calculate oscillator strengths in both the dipole length and velocity approximations (f_L, f_V) when only (π, π^*) configurations are included. The molecular transition moments in the general case are obtained from the dipole length operator only, including the crucial intraatomic terms between $2s$ and $2p$ orbitals.

Systems with open shell configurations as ground states will be calculated in the Grand Canonical Hartree-Fock (GCHF) approximation [8]. The modifications to the SECI and TDHF equations for the transition energies and moments are given by Jørgensen [9].

Since the calculations for the excited states are carried out at the fixed ground state geometry, the parametrization should, in order to be consistent with the Born-Oppenheimer separation [10], describe the vertical Franck-Condon peak, and not, as in CNDO/S [11], the adiabatic $0 \rightarrow 0$ peak. Following the proposal by Pariser [12], the one-center Coulomb integrals are approximated by

$$(r_A r_A | s_A s_A) = I_A - E_A = \gamma_{AA} \tag{2}$$

I_A and E_A representing a properly chosen valence state ionization potential and electron affinity of atom A; we use here the average valence shell values given by Sichel and Whitehead [13] and evaluate then the two-center integrals $(r_A r_A | s_B s_B) = \gamma_{AB}$ by means of the Mataga-Nishimoto interpolation formula [14].

The one-electron atomic parameters are expanded as

$$h_{r_A r_A} = U_{r_A r_A} - \sum_{B \neq A} Z_B \gamma_{AB} \tag{3}$$

where Z_B is the core charge of atom B, and $U_{r_A r_A}$ is the matrix element over the local core-Hamiltonian and contains $(I_A + E_A)$, γ_{AA}, and the Slater-Condon parameters F_A^2 and G_A^1. The one-center exchange integrals $(r_A s_A | s_A r_A)$, differentiating INDO from CNDO, are also expressed in terms of the Slater-Condon parameters and since these were already fitted to experimental atomic energy splittings in the Pople parametrized INDO version, they are carried over to INDO/S unchanged; the exact expressions and values can be found in Ref. [1]. The important distinction between excited and ground state parametrizations of NDO models lies really in the handling of the two-center resonance terms β_{rs}. Local screening in the strength of the π-type interactions can, as originally proposed by Del Bene and Jaffé in their CNDO/S model [11], be effectuated through a reduction of the π-component of the overlap integral S_{rs}

$$\beta_{rs} = 0.5(\beta_A^0 + \beta_B^0)(S_{rs}^\sigma + k S_{rs}^\pi) \tag{4}$$

Ridley and Zerner have performed INDO calculations with such screening plus enhanced σ interactions [15], and Lipari and Duke obtain a similar effect by the choice of different β_A^0 values for s- and p-orbitals together with large Slater exponents [16]. We prefer to treat k as a parameter k_{AB} dependent on the two atoms in question. The splitting of the overlap integral is performed in a local diatomic coordinate system defined by the "bond" between A and B, so rotational invariance is still preserved [17]. Standard Slater exponents are used for the calculation of S_{rs} together with the reparametrized CNDO/S values for the atomic parameters β_A^0 [18].

Numerous calculations with the choice of parameters described above were carried out on the test molecules benzene, formaldehyde, benzonitrile, and the benzonitrile anion to find k_{AB} values, which in a SECI calculation would optimally

describe the vertical UV-spectra [19]. The resulting values are $k_{CC}=0.57$, $k_{CO}=0.75$, and in the closed-shell cyano group containing molecules a k_{CN} value of 0.585; for open-shell systems a value of 0.50 was to be preferred. No calculations were done to obtain an optimal k_{NN} value, the value to be used here is 0.585, unchanged from CNDO/S. These calculations have given satisfactory agreement with experiment for both the UV and PES spectra of the test molecules and for ground state properties resulting from the charge distribution, e.g. the dipole moments [20]. A slightly different parameter set has produced successful results for the optical spectra, singlet–triplet splittings, and photochemical properties of cyclic dienones as well [21]. The transition energies are normally slightly too small in TDHF due to the introduction of correlation in the excited states, but the improvement in the calculated oscillator strengths has been clearly demonstrated; in benzene, for example, the obtained values for the allowed $A_g \rightarrow E_{1u}$ transition are 1.06 in SECI and 0.73 in TDHF, while the experimental value is 0.69 [22].

3. $TCNQ^0$, $TCNQ^-$, and $TCNQ^{2-}$

To demonstrate some strengths and weaknesses of INDO/S, we present in this section results for static and dynamic properties of the neutral tetracyanoquinodimethane (TCNQ) molecule and its singly and doubly charged anion. Ground state results using the original INDO parameters of Pople et al. [1] will also be given in some cases for comparison purposes. Several ground state calculations on TCNQ have been published, ranging from *ab initio* [23, 24] to X_α [25] and semi-empirical methods [26]; the UV-accessible states have mostly been treated in a π-electron-only framework [27, 28]. Recently, however, Lipari et al. [29] extended their CNDO/S2 model to the calculation of the PES and UV spectra of the neutral TCNQ molecule, specifically adjusting the nitrogen parameters so as to obtain agreement with the *ab initio* calculations for the symmetries and splittings of the four highest MO's.

The geometries of $TCNQ^0$ and $TCNQ^-$ were taken from the X-ray crystallography studies of Trueblood [30] and Fritchie [31], respectively. Two geometries were constructed for $TCNQ^{2-}$, the first as an extrapolation of the $TCNQ^0$–$TCNQ^-$ geometries based on monotonic changes upon reduction, the second based on the π bond-order–bond-length formula for carbon–carbon bonds

$$R_{C=C}=1.51\ \text{Å}-0.17\ \text{Å}p_i \tag{5}$$

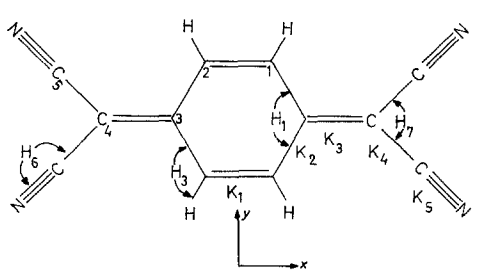

Fig. 1. Coordinate axes, atom labelling system, and internal symmetry coordinate notation (K, H) in the TCNQ species

with p_i, $R_{C\equiv N}$, and R_{C-H} at the values from the first geometry. This last geometry shows considerably longer carbon–carbon distances, except for the C_2–C_3 distance which is slightly shortened; see Fig. 1 for the numbering convention and the coordinate axes. D_{2h} symmetry was imposed, so only states for which the symmetry product with the ground state is $b_{1u}(z)$, $b_{2u}(y)$, or $b_{3u}(x)$ can be reached in a dipole-allowed electronic transition.

3.1. Ground State Results

The ordering and energies of the higher occupied and lower unoccupied molecular orbitals in $TCNQ^0$ calculated with the present INDO/S model are shown in Table 1, along with INDO, CNDO/S2 [29], *ab initio* [23], and experimental [32] results. The PES spectra (gas phase [32] and polarization energy corrected solid state [29]) show a sharp peak at 9.61 eV and a somewhat broader peak centered around 11.3 eV, a very large, structured, and broad peak between 12.3 eV and 13.8 eV, as well as smaller peaks centered around 14.5 eV and 15.8 eV. The overall agreement between these ionization potentials and the INDO/S orbital energies is satisfactory, when an empirical scaling correction has been applied to bring the energy of the HOMO to coincide with the first experimentally observed IP. The second peak at 11.3 eV is assigned to contain two transitions from π_z orbitals, calculated at too large an energy, about 0.8 eV, as found also in the CNDO/S2 calculation. Only the higher-lying $b_{3g}(\pi_z)$ MO is correlated with this peak in the *ab initio* calculations [23, 24], however, the experimental intensities of the first and second peak seem to fit better with the present interpretation. Altogether eight transitions correspond to the large peak in the 12–14 eV area, the calculated width ($\approx$ 1.3 eV) and the experimental width ($\approx$ 1.5 eV) agree quite favorably. After the scaling and still invoking Koopmans' theorem, a closer comparison to the maxima identified in the gas phase spectrum reveals these MO's to be about 0.4–0.5 eV too bound. A tentative assignment would then be an in-plane $\pi_{x,y}$ orbital from the C≡N bonds to each one of the peaks at 12.41 eV and 12.68 eV, the two remaining $\pi_{x,y}$ orbitals at 12.90 eV, and the next four orbitals to the peak around 13.4 eV. Four σ MO's are then assigned as being responsible for the peak at 14.5 eV. Our INDO results and the CNDO/2 results of Ikemoto *et al.* [32] are seen to be quite quite contrary to the above. The π molecular orbitals are too binding with these ground state parametrizations as seen previously for example in the case of benzene [20] and plunge incorrectly far down in the σ manifold, neither agreeing with *ab initio* results nor rendering detailed PES assignments possible.

A comparison of the orbital ordering in the INDO/S and *ab initio* calculations shows complete agreement with the affinity level, which is the $b_{2g}(\pi^*)$ MO positioned far lower than the remaining unoccupied orbitals, and the five highest occupied MO's (the three π_z and two $\pi_{x,y}$ orbitals). Overall, the ordering of the occupied π_z orbitals is exactly the same and the σ levels only need two interchanges within the first fifteen orbitals to exhibit the same ordering. The $b_{1u}(\pi)$–$b_{2g}(\pi^*)$ separation is 5.06 eV in $TCNQ^0$ but reduces to 3.08 eV in $TCNQ^-$ and 1.63 eV in $TCNQ^{2-}$. PES experiments on $Cs_2(TCNQ)_3$ by Schechtman *et al.* indicate that

Table 1. MO ordering and energies ε(eV) in $TCNQ^0$

INDO/S			Exptl.[b]	CNDO/S2[c]		INDO		*Ab initio*[d]	
	$-\varepsilon$	IP[a]	IP		$-\varepsilon$		$-\varepsilon$		$-\varepsilon$
$b_{1u}(\pi^*)$	0.46					$b_{1u}(\pi^*)$	−4.00	$a_u(\pi^*)$	−1.89
$b_{2g}(\pi^*)$	2.79					$b_{2g}(\pi^*)$	0.80	$b_{2g}(\pi^*)$	1.98
$b_{1u}(\pi)$	7.85	9.61	9.61	$b_{1u}(\pi)$	9.54	$b_{1u}(\pi)$	9.65	$b_{1u}(\pi)$	9.52
$b_{3g}(\pi)$	10.32	12.08	11–12	$b_{3g}(\pi)$	11.80	$b_{1g}(\pi)$	13.28	$b_{3g}(\pi)$	12.06
$b_{2g}(\pi)$	10.51	12.27		$b_{2g}(\pi)$	11.88	a_g	14.14	$b_{2g}(\pi)$	12.53
b_{1g}	11.12	12.88	12.41	b_{1g}	13.03	b_{2u}	14.49	b_{1g}	14.11
b_{2u}	11.33	13.09	12.68	a_g	13.40	$b_{2g}(\pi)$	14.95	b_{2u}	14.14
b_{3u}	11.52	13.28	12.90			b_{3u}	14.99	$a_u(\pi)$	14.50
a_g	11.52	13.28				$b_{3g}(\pi)$	15.47	$b_{3g}(\pi)$	14.51
b_{2u}	12.01	13.77	13.30			b_{1g}	15.76	b_{3u}	14.53
b_{1g}	12.12	13.88	13.38			a_g	16.49	a_g	14.68
$a_u(\pi)$	12.38	14.14	13.53			b_{3u}	16.99	$b_{1u}(\pi)$	15.02
$b_{3g}(\pi)$	12.38	14.14				b_{2u}	17.15	b_{1g}	15.36
a_g	12.82	14.58				b_{1g}	17.31	b_{2u}	16.13
b_{1g}	12.82	14.58	14–15			$a_u(\pi)$	17.89	b_{1g}	16.24
b_{3u}	13.00	14.76				$b_{3g}(\pi)$	17.91	a_g	16.28
b_{1u}	13.07	14.81				a_g	18.03	b_{3u}	16.33

[a] Scaled to match HOMO to first exptl. IP. [b] Gas phase spectrum of Ref. [32].
[c] Ref. [29]. [d] Ref. [23].

this level separation is at least 3 eV in $TCNQ^0$ and is reduced by at least 2 eV upon formation of the mono-anion [33]. The orderings for $TCNQ^-$ and $TCNQ^{2-}$ are essentially identical to the one presented for $TCNQ^0$, a couple of π orbitals (a_u, b_{3g}) are shifted up in front of two σ orbitals in $TCNQ^-$, but the ordering within the π- and σ-systems is unchanged.

The calculated net charges and π bond orders are shown in Tables 2 and 3. The INDO parametrizations fail in assigning any polarity to C–H bonds, while *ab initio* methods predict the hydrogens to carry a considerable positive charge [23, 24]. INDO/S tends to give more polar bonds than INDO, which is normally considered to produce decent charge distributions; the differences are fairly small ($\approx$0.05 e^-) and the bond order matrices look quite similar. In general, INDO/S seems to perform better in describing the ground state electronic distribution than CNDO/S, probably partly because of the fit to vertical transitions, which correspond to the ground state equilibrium geometries. The added electrons occupy the $b_{2g}(\pi)$ orbital, which is quite delocalized over the whole molecule, e.g., the atomic orbital coefficients for this orbital in $TCNQ^{2-}$ are 0.45 on C_4, 0.30 on N, 0.25 on C_2 and C_3, and 0.08 on C_5. Rearrangements in the lower-lying MO's lead to more moderate increases in charge on C_4 than could be expected from these coefficients, about 0.12 e^- go on each methide carbon and about 0.11 e^- on each nitrogen for every electron added to $TCNQ^0$. The charge changes in both calculations compared in Table 2 are similar and parallel the corresponding *ab initio* changes [23, 24]. The magnitude of the charges varies drastically between the semiempirical

Table 2. Ground state net charges in $TCNQ^0$, $TCNQ^-$, and $TCNQ^{2-}$

	$TCNQ^0$		$TCNQ^-$		$TCNQ^{2-}$	
Atoms	INDO/S	INDO	INDO/S	INDO	INDO/S[a]	INDO[a]
H	0.03	0.01	0.00	−0.03	−0.03 (−0.04)	−0.07 (−0.10)
C_2	0.00	0.01	−0.03	−0.02	−0.06 (−0.02)	−0.04 (−0.05)
C_3	0.07	0.07	0.05	0.07	0.02 (0.08)	0.06 (0.09)
C_4	0.06	0.01	−0.06	−0.14	−0.19 (−0.21)	−0.28 (−0.30)
C_5	0.18	0.13	0.16	0.15	0.15 (0.17)	0.16 (0.18)
N	−0.27	−0.19	−0.38	−0.31	−0.49 (−0.46)	−0.44 (−0.42)

[a] Values obtained with the bond order–bond length geometry are in parentheses.

Table 3. Ground state π bond orders in $TCNQ^0$, $TCNQ^-$, and $TCNQ^{2-}$

	$TCNQ^0$		$TCNQ^-$		$TCNQ^{2-}$	
Bond	INDO/S	INDO	INDO/S	INDO	INDO/S[a]	INDO[a]
C_1–C_2	0.876	0.879	0.784	0.786	0.707 (0.687)	0.706 (0.685)
C_2–C_3	0.367	0.363	0.491	0.484	0.586 (0.610)	0.585 (0.605)
C_3–C_4	0.781	0.782	0.575	0.590	0.403 (0.359)	0.405 (0.375)
C_4–C_5	0.294	0.302	0.396	0.372	0.447 (0.450)	0.438 (0.434)
C_5–N	0.950	0.950	0.899	0.915	0.868 (0.870)	0.875 (0.878)

[a] Results with the bond order–bond length geometry in parentheses.

and the *ab initio* calculations, but the sign for some of the larger net charges differ even between the two *ab initio* calculations, illustrating the danger in placing too much emphasis on the size of the charges; relative changes are clearly more apt for interpretation.

The potential energy distribution for the totally symmetric normal modes (Fig. 1) in TCNQ has been published [34] and may serve as weighting factors in computing relevant π bond order changes for the process $TCNQ^0 + e^- \rightarrow TCNQ^-$ to be used in a comparison with the frequency changes for stretching modes as observed in the resonance Raman spectroscopy experiments by Jeanmaire and Van Duyne [35] (Table 4). In so doing, one makes the tacit assumption that the normal mode scheme for the ion is the same as that for the neutral parent. This assumption is, in general, incorrect, and will result in some errors in the transition from bond order changes to normal mode changes. The alternative, however, entails performing another normal mode analysis for the ion. We therefore use the normal mode assignment both for the ions and, later, for the excited states. Angle bending coordinates are assigned a weight of zero, based on the very small frequency changes observed for nearly pure bending modes [35]. With the exception of the highly mixed ν_3 mode for which the energy distribution might also be poorly determined, the sign of the frequency changes and their relative positions are

Table 4. Frequency and weighted π bond order changes for reduction of TCNQ

Normal mode	Pot. en.[a] dist. (%)	$\sum K_i \Delta p_i$	$\Delta \nu_i$ cm^{-1}[b]	$\sum K_i \Delta p_i^1$[c]	$\sum K_i \Delta p_i^1$[d]	$\Delta \nu_i^1$ cm^{-1}[b]
ν_2	$K5(87)$	−0.044	−31	−0.026	−0.025	−90
ν_3	$H3(20)$, $K1(46)$, $K2(25)$, $K3(22)$	−0.057	+10	−0.050	−0.064	+ 1
ν_4	$K1(30)$, $K3(59)$	−0.149	−64	−0.125	−0.166	−89
ν_6	$K2(45)$, $K4(21)$	0.077	+28	0.054	0.073	
ν_7	$K2(32)$, $K4(17)$	0.057	+17	0.040	0.054	
ν_8	$K4(23)$, $H6(43)$, $H7(18)$	0.024	+14	0.012	0.018	

[a] See Fig. 1 for the internal symmetry coordinate notation (K, H) and Ref. [34] for the potential energy distribution. $\Delta p_i = p_i(\text{TCNQ}^-) - p_i(\text{TCNQ})$, $\Delta p_i^1 = p_i(\text{TCNQ}^{2-}) - p_i(\text{TCNQ}^-)$.

[b] Ref. [35].

[c] Extrapolated TCNQ–TCNQ$^-$ geometry used for TCNQ^{2-}.

[d] Bond order–bond length TCNQ^{2-} geometry.

correct for both positive and negative changes; no apparent quantitative relationship between the bond order changes and the observed frequency changes seems to exist, neither in INDO/S or INDO.

The use of overlap populations calculated by a Mulliken type of analysis [36] does not change this picture, no matter whether π overlap populations or total overlap populations between the atoms are considered. The π bonding in the classical double and triple bonds is weakened in the anions, drastically so for the C_3–C_4 bonds and more moderately for the C_1–C_2 and C_5–N bonds; the formal single bonds C_2–C_3 and C_4–C_5 gain π bonding, so much that the π character of these bonds in TCNQ^{2-} is actually larger than that of C_3–C_4 (Table 3). The ring skeleton takes on a more benzenoid shape as the C_1–C_2 and C_2–C_3 bond lengths approach each other. That the C_1–C_2 distance remains essentially constant, or maybe even contracts as the X-ray structures indicate, upon anion formation despite the loss of π bonding must be the result of reorganization in the bonding MO's of the ring, strengthening the σ bonding.

The weighted bond order changes for the processes $\text{TCNQ}^- + e^- \rightarrow \text{TCNQ}^{2-}$ are also in Table 4, and on this basis we would expect the same sign for the frequency changes as in the formation of the monoanion. The absolute magnitude of the frequency changes should, if the weighting factors from the normal mode analysis stay constant and are appropriate scaling factors, be somewhat smaller than for monoanion formation according to the extrapolated TCNQ^{2-} model and similar or larger according to the bond-order–bond-length model. The last model seems to be more in accord with the available experimental data.

3.2. Excited State Properties

The vertical transition energies and their oscillator strengths predicted by the INDO/S method are given in Tables 5–7. In solution TCNQ^0 shows one large peak with a maximum at 3.10–3.15 eV [27, 28] and an oscillator strength of

0.93 [28]. The solid state spectrum of Lipari *et al.* [29] shows two dipole-allowed transitions at 3.8 eV and 7.0 eV plus a monopole peak at 5.3 eV. The calculated results are in excellent agreement with these data. Besides, the dipole-allowed transitions shown in Table 5, we also calculate two states of B_{1g} symmetry at 4.19 and 4.47 eV as well as two A_g transitions at 4.43 and 5.37 eV; these are all buried under the tail of the 3.12 eV peak except maybe the A_g state at 5.37 eV, which fits well with the observed monopole transition. The agreement for $TCNQ^-$ is fair, except for the lowest transition predicted 0.75 eV too high. This discrepancy does not change significantly with other choices of two-electron integrals or screening parameters. Examination of the SECI coefficients shows this state to be a mixture of essentially two configurations, 83% of the configuration arising from the promotion of an electron from the doubly occupied $b_{1u}(\pi)$ orbital to the singly occupied $b_{2g}(\pi)$ orbital and 16% of the configuration involving the promotion of the unpaired electron into the empty $b_{1u}(\pi^*)$ orbital. The state at 2.81 eV is mostly this last HOMO–LUMO transition, which is predicted at a slightly too low energy compared to experiment. A possible explanation for both results is that the minimal basis set in conjunction with the use of the GCHF procedure does not make the half-filled level bonding enough, i.e., the orbital is still too close to the virtual orbitals, despite the 2 eV reduction in the b_{1u}–b_{2g} spacing. There is very strong mixing among the higher-lying (π, π^*) and (σ, σ^*) states; as a matter of fact, in the higher states there are about 15 configurations with SECI coefficients larger than 0.1. The ratio of oscillator strengths of the two lowest transitions is in very good agreement with recent experimental results [37], and sharp disagreement with PPP-type calculations [27, 28]. The positioning of the B_{1u} states lowest, and the very weak transition to the A_u state, also agree with experiment [37].

Table 5. Vertical transitions (eV) and their oscillator strengths in TCNQ

		SECI			TDHF			Litt.[b]	
Sym	# Config.[a]	E	f_L	f_V	E	f_L	f_V	E	f_L
B_{3u}	18	3.12	1.9227	0.7660	2.92	1.3049	1.3042	3.06[c]	1.91[c]
B_{3u}	18	5.99	0.0823	0.0607	5.97	0.0573	0.0576	3.22[d]	1.59[d]
B_{2u}	14	6.13	0.0346	0.0205	6.12	0.0414	0.0419	3.29[e]	1.77[e]
B_{2u}	14	6.26	0.2766	0.1863	6.24	0.2676	0.2680		
B_{3u}	30	3.10	1.8357		2.89	1.2414			
B_{1u}	11	5.15	0.0034		5.14	0.0032			
B_{1u}	11	5.42	0.0009		5.41	0.0008			
B_{2u}	26	5.65	0.1301		5.57	0.1116			
B_{3u}	30	5.87	0.0111		5.82	0.0053			
B_{2u}	26	6.19	0.0549		6.17	0.0479			

[a] There are 64 (π, π^*) configurations, out of which 18 are of B_{3u} symmetry and 14 of B_{2u} symmetry.

[b] All values refer to the lowest B_{3u} state.

[c] Ref. [27] (PPP-model).

[d] Ref. [28] (PPP-model).

[e] Ref. [29] (CNDO/S2-model).

Table 6. Vertical transitions (eV) and their oscillator strengths in $TCNQ^-$

		SECI			TDHF			Exptl.	
Sym	# Config.[a]	E	f_L	f_V	E	f_L	f_V	E[b]	f[b]
B_{1u}	20	2.20	0.7982	0.0675	2.13	0.3711	0.3711		
B_{1u}	20	2.85	0.2180	0.0153	2.69	0.7545	0.7545		
A_u	16	2.99	0.0033	0.0089	2.94	0.0235	0.0235		
A_u	16	3.79	0.0034	0.0030	3.76	0.2819	0.2819		
B_{1u}	20	5.23	0.0011	0.0002	5.19	0.0193	0.0193		
A_u	16	5.48	0.2329	0.1619	5.48	0.0864	0.0863		
B_{1u}	36	2.19	0.7840		2.10	0.3914		1.45	0.28
B_{1u}	36	2.81	0.1496		2.66	0.6430		2.84	0.45
A_u	34	2.98	0.0032		2.92	0.0222			
A_u	34	3.62	10^{-5}		3.55	0.1942			
A_u	34	4.79	0.0635		4.71	0.0020		4.45	0.023
B_{1u}	36	5.00	0.0450		4.87	0.0177		4.74	0.023
B_{1u}	36	5.39	0.0049		5.34	0.0420		5.32	0.10

[a] There are 71 (π, π^*) states, out of which 20 are of B_{1u} symmetry and 16 of A_u symmetry. Three B_{3u} states lie at 3.10, 4.76, and 4.97 eV with $f \sim 10^{-4}$.

[b] Two lowest transitions from Ref. [37], remaining results from Ref. [28].

Table 7. Vertical transitions (eV) and their oscillator strengths in $TCNQ^{2-}$

	SECI			TDHF			Exptl.[b]	
Sym	E	f_L	f_V	E	f_L	f_V	E	f
B_{3u}	3.02	1.0744	0.7350	2.96	0.8986	0.8986		
B_{2u}	3.09	0.0588	0.0046	3.00	0.0452	0.0452		
B_{2u}	4.28	0.7766	0.4431	4.23	0.6511	0.6492		
B_{3u}	5.80	0.0874	0.0617	5.71	0.0921	0.0929		
B_{2u}	5.96	0.0342	0.0061	5.88	0.0623	0.0620		
B_{2u}	6.11	0.4509	0.2638	6.09	0.3487	0.3448		
B_{3u}	6.38	0.1528	0.1315	6.35	0.1520	0.1518		
B_{2u}	3.15	0.0401	0.0014	3.06	0.0318	0.0318		
B_{3u}	3.25	0.9392	0.6725	3.20	0.8107	0.8100	3.75	0.54
B_{2u}	4.19	0.8574	0.4811	4.13	0.7154	0.7161	5.16	0.30
B_{2u}	5.72	0.0357	0.0054	5.63	0.0797	0.0796		
B_{3u}	5.73	0.1221	0.0784	5.63	0.1120	0.1123		
B_{2u}	5.85	0.4434	0.2477	5.83	0.3225	0.3225	5.90	0.53
B_{3u}	6.19	0.2344	0.1608	6.13	0.2453	0.2451		

[a] The extrapolated geometry is used for the top results, the bond order–bond length geometry for the lower results. Only (π, π^*) configurations were included, 15 of B_{2u} and 17 of B_{3u} symmetry.

[b] Ref. [38]. The oscillator strengths were calculated from the published spectrum.

An improved account of the UV-spectrum of $TCNQ^{2-}$ has recently been given by Suchanski and Van Duyne, showing that previously published spectra were contaminated by decay products with O_2 [38]. The calculated results are in agreement with the new spectrum (Table 7) with respect to the number of intense peaks (3), but the energies are significantly below the experimental values. A similar effect as in $TCNQ^-$ suggests itself; also, no account is taken of possible reorganization in the excited state and changes in correlation energy. The discrepancies are smallest for the bond-order–bond-length geometry, most likely because this geometry is more benzenoid than the extrapolated geometry.

There is also a possible discrepancy caused by the environment: our calculations consider an isolated species, whereas the experiments were performed in an ionic solid or strongly polar liquids. The polarization due to the dianion will certainly change total energies and will stabilize the ground state, rather than the excited states which cannot relax on a timescale of 10^{-15} seconds. We therefore expect an isolated-molecule calculation to underestimate the excitation energies observed in a polarizable medium, and furthermore expect this underestimate to increase with charge.

The changes in π bond orders upon excitation of $TCNQ^-$ are shown in Table 8, together with available experimental vibrational frequency changes. The correlation to the first excited state is satisfactory, and we predict that if the second doublet at 2.85 eV was excited, small vibrational frequency changes would result in this state compared to the ground state, except for ν_2. A sign change should occur for the changes in ν_6 and ν_7, compared to the changes in the lowest excited doublet. The corresponding calculated values in the first excited state of $TCNQ^0$ and $TCNQ^{2-}$ are given in Table 9; large negative shifts ought to be observed for ν_2 and in particular ν_4 in $TCNQ^0$, more moderate positive changes are predicted for ν_6, ν_7, and ν_8. In $TCNQ^{2-}$ we would expect large changes in the frequencies of the ν_4, ν_6, and ν_7 modes when measured by resonance Raman spectroscopy in the state with large oscillator strength at 3.25 eV. The excited states of $TCNQ^{2-}$ show large charge reorganizations, while no low-lying states in $TCNQ^0$ or $TCNQ^-$ display changes of more than 0.005 e^- on one atom, e.g., the lowest state in $TCNQ^{2-}$

Table 8. Frequency and π bond order changes upon excitation of $TCNQ^-$

Bond	Δp_i	Δp_i^1	Mode	$\sum K_i \Delta p_i$	$\Delta \nu_i\,\mathrm{cm}^{-1}$ [a]	$\sum K_i \Delta p_i^1$
C_1–C_2	−0.080	0.026	ν_2	−0.022	−42	−0.018
C_2–C_3	0.068	−0.052	ν_3	−0.053	0	−0.002
C_3–C_4	−0.152	−0.007	ν_4	−0.113	−54	−0.004
C_4–C_5	0.038	0.006	ν_6	0.038		−0.022
C_5–N	−0.026	−0.020	ν_7	0.028		−0.016
			ν_8	0.009		0.001

$\Delta p_i = p_i(TCNQ^-(^2B_{1u})) - p_i(TCNQ^-(^2B_{2g}))$, $E = 2.20$ eV
$\Delta p_i^1 = p_i(TCNQ^-(^2B_{1u})) - p_i(TCNQ^-(^2B_{2g}))$, $E = 2.85$ eV
[a] Ref. [35].

Table 9. π bond order changes upon excitation of $TCNQ^0$ and $TCNQ^{2-}$

Bond	Δp_i	Δp_i^1	Mode	$\sum K_i \Delta p_i$	$\sum K_i \Delta p_i^1$
C_1–C_2	−0.126	0.092	ν_2	−0.028	−0.007
C_2–C_3	0.119	−0.169	ν_3	−0.075	0.016
C_3–C_4	−0.213	0.072	ν_4	−0.163	0.070
C_4–C_5	0.058	−0.031	ν_6	0.066	−0.083
C_5–N	−0.032	−0.008	ν_7	0.048	−0.059
			ν_8	0.013	−0.007

$\Delta p_i = p_i(TCNQ^0(^1B_{3u})) - p_i(TCNQ^0(^1A_g))$, $E = 3.12$ eV
$\Delta p_i^1 = p_i(TCNQ^{2-}(^1B_{3u})) - p_i(TCNQ^{2-}(^1A_g))$, $E = 3.25$ eV

shows 0.17 e^- being pushed onto the C_1 and C_2 atoms in the ring from the methide carbons in particular.

4. Discussion

The results given in Sect. 3 show that properties of the closed-shell neutral TCNQ species are computed quite satisfactorily within the INDO/S model; in particular, the absorption spectrum is described far better than in any of the previous semi-empirical studies, both transition probabilities and frequencies are quite satisfactory. For the charged TCNQ species, the agreement is far worse; some of this is undoubtedly due to uncertainties in the geometry of the molecule, but a good deal must arise from the presence of a substantial amount of negative charge on the molecule. The strength of screening in any many-electron system is a function of the local electron density; in the electron gas, the screening becomes so effective at high density that the effective potential becomes of the Yukawa form $r^{-1}e^{-\alpha r}$, instead of the Coulomb form r^{-1}. To model this behaviour is, however, quite difficult in a molecular system which is neither homogeneous nor quasi-isotropic, but instead is characterized by sharp spatial charges in the Coulomb potential. We feel that highly-charged systems will require different parametrization from the neutral species, as suggested by our results on $TCNQ^{2-}$.

The Grand Canonical SECI and TDHF procedures applied to the INDO/S model Hamiltonian seem unsatisfactory for frequencies (although the oscillator strengths are quite good), when the excited state contains contributions from partial occupation of several virtual orbitals of differing symmetry. In view of the nature of the GC scheme, which essentially splits each electron into two halves of opposite spin component, this difficulty is not unreasonable – the exchange terms, in particular, should differ considerably from the results of a proper spin-projected doublet calculation. In all cases the TDHF method clearly provides the superior description of the intensities. Despite the introduction of non-nearest neighbor β_{rs} terms in the evaluation of f_V, the equivalence between f_L and f_V obeyed in, e.g., PPP calculations is observed here to better than 1% too, when all the (π, π^*) configurations are considered.

The attempt to correlate resonance Raman frequency changes with change in bond order seems generally to fail; although there is a qualitative correspondence, no quantitative conclusions may be drawn. Considering that frequency changes generally are very poorly described even in accurate *ab initio* SCF calculations, this is perhaps not too surprising. A major part of the errors is believed to come from the lack of potential energy distributions for the anions and excited states; notably due to geometry changes, the normal mode analysis for ground state $TCNQ^0$ cannot be expected to hold accurately in these cases.

The INDO/S procedure represents another semiempirical method designed for rapid, easy calculation of interesting properties (principally dynamic, but also static charge distributions) of medium-sized molecules containing first-row atoms. For certain systems the procedure gives very satisfactory results, while other systems are less tractable. We have suggested causes for these inaccuracies, and which sorts of molecules should present the most serious difficulties.

Acknowledgements. We are grateful to David Beveridge for helpful comments on the INDO model. We thank Professor Max Goldstein of the ERDA Courant Computation Center at New York University for generous amounts of computer time and friendly conversations. MR thanks R. van Duyne for prepublication copies of Refs. [35] and [38]. We are indebted to Paul Gans and Jens Eriksen for helpful conversations.

References

1. Pople, J. A., Beveridge, D. L.: Approximate molecular orbital theory. New York: McGraw-Hill 1970
2. Linderberg, J., Öhrn, Y.: Propagators in quantum chemistry. London: Academic Press 1973
3. Franck, J.: Trans. Faraday Soc. **21**, 536 (1925); Condon, E. U.: Phys. Rev. **32**, 858 (1928)
4. Koopmans, T.: Physica **1**, 104 (1934)
5. Murrell, J. N., Kettle, S. F. A., Tedder, J. M.: Valence theory. London: Wiley 1965
6. Jørgensen, P., Linderberg, J.: Intern. J. Quantum Chem. **4**, 587 (1970)
7. Linderberg, J.: Chem. Phys. Letters **1**, 39 (1967)
8. Abdulnur, S. F., Linderberg, J., Öhrn, Y., Thulstrup, P. W.: Phys. Rev. **A6**, 889 (1972)
9. Jørgensen, P.: J. Chem. Phys. **57**, 4884 (1972)
10. Born, M., Oppenheimer, J. R.: Ann. Physik **84**, 457 (1927)
11. Del Bene, J., Jaffé, H. H.: J. Chem. Phys. **48**, 1807 (1968); **48**, 4050 (1968); **49**, 1221 (1968); **50**, 563 (1969); **50**, 1126 (1969)
12. Pariser, R., Parr, R. G.: J. Chem. Phys. **21**, 767 (1953)
13. Sichel, J. A., Whitehead, M. A.: Theoret. Chim. Acta (Berl.) **7**, 32 (1967)
14. Mataga, N., Nishimoto, K.: Z. Physik. Chem. **13**, 140 (1957)
15. Ridley, J. E., Zerner, M. C.: Theoret. Chim. Acta (Berl.) **32**, 11 (1973); J. Mol. Spectry. **50**, 457 (1974); Theoret. Chim. Acta (Berl.) **42**, 223 (1976)
16. Lipari, N. O., Duke, C. B.: J. Chem. Phys. **63**, 1748 (1975); **63**, 1768 (1975)
17. Schulte, K. W., Schweig, A.: Theoret. Chim. Acta (Berl.) **33**, 19 (1974)
18. Ellis, R. L., Kuehnlenz, G., Jaffé, H. H.: Theoret. Chim. Acta (Berl.) **26**, 131 (1972)
19. Krogh-Jespersen, K.: Ph.D. Thesis. New York University 1976
20. Krogh-Jespersen, K., Ratner, M. A.: J. Chem. Phys. **65**, 1305 (1976)
21. Eriksen, J., Krogh-Jespersen, K., Ratner, M. A., Schuster, D. I.: J. Am. Chem. Soc. **97**, 5596 (1975)
22. Kearns, D. R.: J. Chem. Phys. **36**, 1608 (1962)
23. Johansen, H.: Intern. J. Quantum Chem. **9**, 459 (1975)

24. Jonkman, H. T., Van Der Velde, G. A., Nieuwpoort, W. C.: Chem. Phys. Letters **25**, 62 (1974)
25. Batra, I. P., Bennett, B. I., Herman, F.: Phys. Rev. B. **11**, 4927 (1975)
26. Ratner, M., Sabin, J. R., Ball, E. E.: Mol. Phys. **26**, 1177 (1973); Ladik, J., Karpfen, A., Stollhoff, G., Fulde, P.: Chem. Phys. **31**, 291 (1975)
27. Jonkman, J., Kommandeur, J.: Chem. Phys. Letters **15**, 496 (1972)
28. Bieber, A., Andre, J. J.: Chem. Phys. **5**, 166 (1974)
29. Lipari, N. O., Nielsen, P., Ritsko, J. J., Epstein, A. J., Sandman, D. J.: Phys. Rev. B **14**, 2229 (1976)
30. Long, R. E., Sparks, R. A., Trueblood, K. N.: Acta Cryst. **18**, 932 (1965)
31. Fritchie, C. J.: Acta Cryst. **20**, 892 (1966)
32. Ikemoto, I., Samizo, K., Fujikawa, T., Ishii, K., Ohta, T., Kuroda, H.: Chem. Letters 785 (1974)
33. Schechtman, B. H., Lin, S. F., Spicer, W. E.: Phys. Rev. Letters **34**, 667 (1975)
34. Girlando, A., Pecile, C.: Spectrochim. Acta **29A**, 1859 (1973)
35. Jeanmaire, D. L., Van Duyne, R. P.: J. Am. Chem. Soc. **98**, 4029 (1976); **98**, 4034 (1976)
36. Mulliken, R. S.: J. Chem. Phys. **23**, 1833 (1955)
37. Haller, I., Kaufman, F. B.: J. Am. Chem. Soc. **98**, 1464 (1976)
38. Suchanski, M. R., Van Duyne, R. P.: J. Am. Chem. Soc. **98**, 250 (1976)

Received August 10, 1976/February 11, 1977/September 26, 1977